Molybdenum–Pterin Chemistry. 2. Reinvestigation of Molybdenum(IV) Coordination by Flavin Gives Evidence for Partial Pteridine Reduction

ARTICLE *in* INORGANIC CHEMISTRY · MAY 1999

Impact Factor: 4.76 · DOI: 10.1021/ic9808798

3 AUTHORS, INCLUDING:

Sharon J Nieter Burgmayer
Bryn Mawr College
48 PUBLICATIONS **810** CITATIONS

Molybdenum−Pterin Chemistry. 2. Reinvestigation of Molybdenum(IV) Coordination by Flavin Gives Evidence for Partial Pteridine Reduction

Heather Layton Kaufmann,[†] Patrick J. Carroll,[‡] and Sharon J. Nieter Burgmayer*[,†]

Department of Chemistry, Bryn Mawr College, Bryn Mawr, Pennsylvania 19010 and Department of Chemistry, University of Pennsylvania, Philadelphia, Pennsylvania 19104

Received July 27, 1998

The coordination of alloxazine and pterins to molybdenum(IV) is demonstrated in this study. The synthesis of $MoOCl_3$(pteridineH), where pteridineH is the protonated form of 1,3,7,8-tetramethylalloxazine (tmaz), 2-pivaloyl-6,7-dimethylpterin (piv-dmp), and 6,7-dimethylpterin (dmp), proceeds readily starting from $Mo(IV)Cl_4(acetonitrile)_2$ and the pteridine ligand in chloroform or methanol. X-ray crystal structures of $MoOCl_3$(tmazH) (**1**) and $MoOCl_3$(piv-dmpH) (**2**) show that Mo chelates each pteridine at the carbonyl oxygen and pyrazine nitrogen and that the pteridine ligand is protonated at the other nitrogen in the pyrazine ring. A third X-ray structure for $MoOCl_3$(H_3-dmp) (**4**) is included in this work since its determination permits the comparison of metrical parameters for the oxidized and reduced forms of a pterin in identical molybdenum coordination environments. The major difference observed in the structures of **2** as compared to **4** is the Mo−N5 bond length which is significantly shorter in compound **4** containing the reduced form of the pterin. Pteridine protonation is facilitated by molybdenum(IV) coordination due to partial reduction of the pteridine ring through electronic delocalization from Mo to the pteridine ligand. Electronic spectroscopy monitoring the solution reactivity of **1**, **2**, and $MoOCl_3$(dmpH) (**3**) provides evidence to support this idea. Solution conditions favoring deprotonation of the complexes **1**−**3** promote pteridine dissociation and complex decomposition.

Introduction

Two decades ago, discoveries of several distinct molybdenum-dependent enzymes[1] foreshadowed our contemporary knowledge about the ubiquitous nature of oxo-molybdoenzymes.[2] At that time the meager information on the molybdenum environment in these enzymes included thiolate coordination and molybdenum redox cycling between oxidation states +6, +5, and +4. It was also recognized that several enzymes were flavoproteins. On this basis Selbin and co-workers initiated an investigation directed at determining if molybdenum coordination by the flavin cofactor would be possible in these enzymes.[3] Their 1974 report concluded that a mono-oxo molybdenum(IV) flavin complex was produced by reactions such as the example illustrated in eq 1.

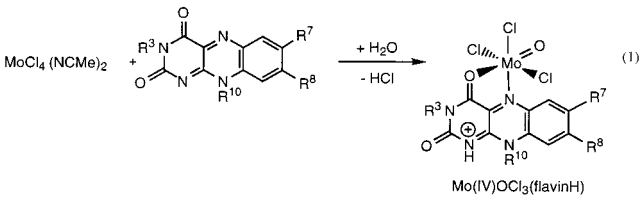

(1)

The molecularity of the product, $Mo(IV)OCl_3$(flavinH), was determined from spectroscopic and microanalytical data. Infrared spectra revealed characteristic absorptions for the oxo ligand on molybdenum and for flavin coordination through the N5 and O4 positions. This research was called into question shortly after its publication.[4] An argument was presented for an alternative interpretation of eq 1 where the product was formulated as $[flavinH]_2[Mo_2O_3Cl_6]$, a salt containing a protonated flavin cation anda dinuclear Mo(V) anion.

Our interest in eq 1 relates to an ongoing project to systematize the compatibility of oxidation states in molybdenum complexes of pteridines. For example, it is observed that Mo(VI), but not Mo(IV), readily reacts with fully reduced tetrahydropterins[5,6] whereas Mo(0)[7] and Mo(IV) yield complexes of oxidized pterins. In contrast, Mo(VI) reacts only sluggishly, if at all, with oxidized pterins.[8] We and others have also observed that molybdenum(VI) coordination to reduced pterins may lead to internal redox reactions producing reduced Mo(IV) and oxidized pterin.[6a,9] In all of these systems the molybdenum−pterin unit is highly delocalized and tends toward acquiring a molybdenum charge consistent with a Mo(V) oxidation state

[†] Bryn Mawr College.
[‡] University of Pennsylvania.

(1) (a) Stiefel, E. I. In *Molybdenum and Molybdenum-Containing Enzymes*; Coughlan, M. P., Ed.; Pergamon Press: New York, 1980; p 43 and other chapters therein. (b) Stiefel, E. I.; Newton, W. E.; Watt, G. D.; Hadfield, K. L.; Bulen, W. A. In Raymond, K. N., Ed.; Advances in Chemistry Series 162; American Chemical Society: Washington, DC, 1977; p 353. (c) Swedo, K. B.; Enemark, J. H. *J. Chem. Educ.* **1979**, *56*, 70.
(2) Hille, R. *Chem. Rev.* **1996**, *96*, 2757.
(3) Selbin, J.; Sherrill, J.; Bigger, C. H. *Inorg. Chem.* **1974**, *13*, 2544.
(4) Sawyer, D. T.; Doub, W. H., Jr. *Inorg. Chem.* **1975**, *14*, 1736.
(5) (a) Burgmayer, S. J. N.; Baruch, A.; Kerr, K.; Yoon, K. *J. Am. Chem. Soc.* **1989**, *111*, 4982. (b) Burgmayer, S. J. N.; Arkin, M. R.; Bostick, L.; Dempster, S.; Everett, K M.; Layton, H. L.; Paul, K. E.; Rogge, C.; Rheingold, A. L. *J. Am. Chem. Soc.* **1995**, *117*, 5812.
(6) (a) Fischer, B.; Schmalle, H.; Dubler, E.; Schäfer, A.; Viscontini, M. *Inorg. Chem.* **1995**, *34*, 5726. (b) Fischer, B.; Strähle, J.; Viscontini, M. *Helv. Chim. Acta* **1991**, *74*, 1544. (c) Fischer, B.; Schmalle, H.; Baumgartner, M.; Viscontini, M. *Helv. Chim. Acta* **1997**, *80*, 103.
(7) Burgmayer, S. J. N.; Kaufmann, H. L.; Fischer, B.; Fortunato, G.; Hug, P. *Inorg. Chem.* **1999**, *38*, xxxx.
(8) Burgmayer, S. J. N.; Stiefel, E. I. *J. Am. Chem. Soc.* **1986**, *108*, 8310.
(9) Kaufmann, H. L.; Burgmayer, S. J. N.; Liable-Sands, L.; Rheingold, A. *Inorg. Chem.* **1999**, *38*, xxxx.

10.1021/ic9808798 CCC: $18.00
Published on Web 00/00/0000 PAGE EST: 6.6

as deduced from XPS measurements.[7] It was in this context that the disputed claim of Mo(IV) complexation by flavin piqued our curiosity.

We have recently reinvestigated one of the reactions reported by Selbin and have verified its original interpretation. In addition to reproducing the synthesis and the spectroscopic data from the 1974 report, an X-ray crystal structure of $MoOCl_3$(tmazH) (**1**) confirms the original formulation. The synthetic method for **1** has been extended to reactions of oxidized pterins with $MoCl_4(NCMe)_2$. Descriptions of these reactions and product characterization including X-ray structural determination and electronic, infrared, and NMR spectroscopy is also presented in this paper. Finally the X-ray structure of $MoOCl_3(H_3dmp)$ (**4**), is included in this report because it provides the opportunity to compare structural differences between molybdenum complexes of reduced and oxidized dimethylpterin.

Experimental Section

All chemicals were purchased from Aldrich unless otherwise noted and used without further purification except as noted below. Solvents of the highest purity available were dried over 4 Å molecular sieves except methanol, which was dried over 3 Å molecular sieves, stored under N_2, and used without further purification. All molybdenum reactions were performed in standard laboratory glassware under a nitrogen atmosphere in a Vacuum Atmospheres drybox. NMR spectra were obtained using an IBM 300 MHz FT-NMR, and chemical shifts are reported in parts per million referenced to internal TMS or solvent. Infrared spectra of samples of KBr disks were recorded on a Perkin-Elmer FT-IR Model 2000 instrument and are referenced to the 1601.4 cm^{-1} absorption of polystyrene. Electronic spectra were recorded using a Hewlett-Packard 8452A spectrophotometer. Solution conductivities were measured using a Barnstead PM-70CB conductivity bridge equipped with a Yellow Springs Instruments 3403 dip cell. Microanalyses were performed by Robertson Microanalytical Labs, Madison, NJ.

1,3,7,8-Tetramethylalloxazine (tmaz). The synthesis is based on the procedure of Selbin et al.[3] Lumichrome (3.08 g, 0.0127 mol), potassium carbonate (10.87 g, mol), methyl iodide (4.47 mL), and acetone (60 mL) were placed in a round-bottom flask and refluxed overnight. The reaction solution was filtered and the solid was washed with acetone. This solid was treated with chloroform to extract additional product. The majority of product was in the filtrate which was evaporated to dryness to yield a yellow solid. This solid was recrystallized from chloroform (1.31 g, 38% combined yield). Product purity was determined by ^{1}H NMR in ($CDCl_3$) δ: 7.78 (1H, s, *H*6), 7.23 (1H, s, *H*9), 3.79 (3H, s, $-CH_3$), 3.57 (3H, s, $-CH_3$), 2.51 (3H, s, $-CH_3$), 2.48 (3H, s, $-CH_3$). Anal. Calcd for $C_{14}H_{14}N_4O_2$: C, 62.21; H, 5.22; N, 20.73. Found: C, 62.07; H, 5.26; N, 20.61.

2-*N*-Pivoloylamido-6,7-dimethylpterin (piv-dmp). 6,7-Dimethylpterin[10] (3.82 g, 20 mmol) and 20 mL of trimethylacetic (pivalic) anhydride were placed in a 100 mL round-bottom flask equipped with a reflux condensor and refluxed in an oil bath for 2 h. The formation of a brownish solid resulted as the flask cooled to room temperature. Ether was added to break up the solid, and the slurry was vacuum filtered. The yellow solid was dried in vacuo over P_2O_5 (4.1 g, 73% yield) and recrystallized from ethanol if necessary (1.9 g, 31% yield). ^{1}H NMR ($CDCl_3$): δ 1.34 (9H, s, $-C(CH_3)_3$); 2.69, 2.71 (3H, s, $-CH_3$-(6), $-CH_3$(7)).

$MoOCl_3$(tmazH) (1). This synthesis is based on the procedure of Selbin et al.[3] A bright yellow solution of tmaz (0.104 g, 0.385 mmol) in chloroform (25 mL) was added dropwise to a stirred purple slurry of $MoCl_4(MeCN)_2$ (0.154 g, 0.482 mmol) in chloroform (25 mL), resulting in an orange brown solution. After stirring overnight, a dark purple solid formed and was isolated, washed with chloroform, methylene chloride, diethyl ether, and dried (0.038 g, 20% yield).

$MoOCl_3$(piv-dmpH) (2). A clear yellow solution of piv-dmp (0.108 g, 0.500 mmol) in chloroform (10 mL) was added slowly dropwise to a stirred brown-purple slurry of $MoCl_4(MeCN)_2$ (0.1597 g, 0.500 mmol) in chloroform (25 mL) with no change in color. After stirring overnight, a dark blue solution had formed and a dark blue/purple solid had precipitated on the bottom of the flask. The solid was collected by filtration, washed with ether, and dried under vacuum (0.25 g, 90% yield). Recrystallization of the complex from acetonitrile by slow diffusion of ether produced crystals suitable for X-ray diffraction. Anal. Calcd for $MoC_{13}H_{18}N_5O_3Cl_3$ $MoOCl_3$(Hpiv-dmp): C, 31.58; H, 3.67; N, 14.16; Cl, 19.05; Mo, 17.18. Found: C, 26.81; H, 3.47; N, 11.03; Cl, 20.75; Mo, 16.72.

$MoOCl_3$(dmpH) (3). A pale yellow slurry of dmp[17] (0.096 g, 0.5 mmol) in methanol (12 mL) was added dropwise to a stirred brown slurry of $MoCl_4(MeCN)_2$ (0.271 g, 0.848 mmol) in methanol (13 mL), resulting in the gradual appearance of a green color to the slurry. A clear very dark green solution was observed after the solution was stirred overnight, indicating that all of the pterin had dissolved. The solution was evaporated until a thick tar remained. Acetonitrile was added to the tar, forming a deep blue solution with a white insoluble precipitate which was allowed to settle. The pale solid was filtered, and the dark blue filtrate was evaporated to dryness. The solid was collected by washing with ether and filtering(0.074 g, 30% yield).

X-ray Crystal Determinations. X-ray intensity data were collected on an Rigaku R-AXIS IIc area detector employing graphite-monochromated Mo Kα radiation (λ = 0.710 69 Å). Indexing was performed from a series of 1° oscillation images with exposures of 30 min per frame. A hemisphere of data was collected using 6° oscillation angles with exposures of 30 min per frame and a crystal-to-detector distance of 82 mm. Oscillation images were processed using bioteX,[11] producing a listing of unaveraged F^2 and $\sigma(F^2)$ values which were then passed to the teXsan[11] program package for further processing and structure solution on a Silicon Graphics Indigo R4000 computer. The intensity data were corrected for Lorentz and polarization effects but not for absorption. The structure was solved by direct methods (SIR92). Refinement was by full-matrix least squares based on F^2 using SHELXL-93.[11] All reflections were used during refinement (F^2's that were experimentally negative were replaced by $F^2 = 0$). The weighting scheme used was $w = 1/[\sigma^2(F_o^2) + 0.0754P^2 + 5.1152P]$, where $P = (F_o^2 + 2F_c^2)/3$. Non-hydrogen atoms were refined anisotropically, and hydrogen atoms were included as constant contributions to the structure factors and were not refined. Table 2 is an abbreviated list of

(10) Mager, H. I. X.; Addink, R.; Berendo, W. *Recl. Trav. Chem.* **1967**, *86*, 833.

(11) bioteX: A suite of Programs for the Collection, Reduction and Interpretation of Imaging Plate Data, Molecular Structure Corporation, 1995. teXsan: Crystal Structure Analysis Package, Molecular Structure Corporation, 1985 and 1992. SIR92: Altomare, A., Burla, M. C., Camalli, M., Cascarano, M., Giacovazzo, C., Guagliardi, A., Polidoro, G. *J. Appl. Crystallogr*. **1994**, *27*, 435. SHELXL-93: Program for the Refinement of Crystal Structures, Sheldrick, G. M. University of Göttingen, Germany, 1993. $R_1 = \sum||F_o| - |F_c||/\sum|F_o|$; $wR_2 = \{\sum w(F_o^2 - F_c^2)^2/\sum w(F_o^2)^2\}^{1/2}$. GOF = $\{\sum w(F_o^2 - F_c^2)^2/(n - p)\}^{1/2}$, where n = the number of reflections and p = the number of parameters refined.

(12) (a) Perkinson, J.; Brodie, S.; Yoon, K.; Mosny, K.; Carroll, P. J.; Burgmayer, S. J. N. *Inorg. Chem.* **1991**, *30*, 719. (b) Bessenmacher, C.; Vogler, C.; Kaim, W. *Inorg. Chem.* **1989**, *28*, 4645. (c) Heilmann, O.; Hornung, F. M.; Kaim, W.; Fiedler, J. *J. Chem. Soc., Faraday Trans.* **1996**, *92*, 4233. (d) Kohzuma, T.; Masuda, H.; Yamauchi, O. *J. Am. Chem. Soc.* **1989**, *111*, 3431. (e) Kohzuma, T.; Odani, A.; Morita, Y.; Takani, M.; Yamauchi, O. *Inorg. Chem.* **1988**, *27*, 3854. (f) Funahashi, Y.; Hara, H.; Masuda, H.; Yamauchi, O. *Inorg. Chem.* **1997**, *36*, 3869. (g) Mitsumi, M.; Toyoda, J.; Nakasuji, K. *Inorg. Chem.* **1995**, *34*, 3367. (h) Hueso-Urena, F.; Jimenez-Pulido, S. B.; Moreno Carretero, M. N.; Quiros-Olozabal, M.; Salas-Peregrin, J. M. *Polyhedron* **1997**, *16*, 607.

(13) Hemmerich, P.; Muller, F.; Ehrenberg, A. In *Oxidases and Related Redox Systems*; King, T. E., Mason, H. S., Morrison, M., Eds.; Wiley: New York, 1965; Vol. 1, pp 157−178.

(14) Abelleira, A.; Galang, R. D.; Clarke, M. J. *Inorg. Chem*. **1990**, *29*, 633.

(15) Clarke, M. J.; Dowling, M. G.; Garafalo, A. R.; Brennan, T. F. *J. Biol. Chem*. **1980**, *255*, 3472.

(16) Burgmayer, S. J. N. In Clarke, M. J., Ed.; Structure and Bonding 92; Springer: Heidelberg; 1998; p 67.

(17) (a) Pierpont, C. *Prog. Inorg. Chem.* **1994**, *41*, 331. (b) Attia, A.; Pierpont, C. *Inorg. Chem.* **1998**, *37*, 3051.

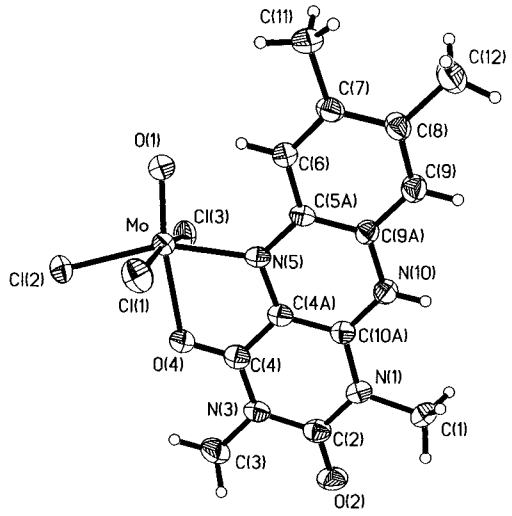

Figure 1. ORTEP drawing of the molecular structure of $MoOCl_3$(tmazH) (**1**) with thermal ellipsoids at 30% probability.

crystallographic information for **1**, **2**, and **4**. Crystals of **1** or **2** suitable for X-ray diffraction were crystallized from slow diffusion of ether into an acetonitrile solution. Refinement of **1** converged to $R_1 = 0.0712$ and $wR_2 = 0.1805$ for 2688 reflections for which $F > 4\sigma(F)$ and $R_1 = 0.0833$, $wR_2 = 0.1895$, and GOF = 1.175 for all 3122 unique, nonzero reflections and 231 variables. The maximum Δ/σ in the final cycle of least squares was −0.001, and the two most prominent peaks in the final difference Fourier were +0.611 and −1.090 e/Å^3. The unit cell of **2** was found to contain diethyl ether as solvent of crystallization. Refinement of **2** converged to $R_1 = 0.0363$ and $R_2 = 0.0949$ for 3938 reflections for which $F > 4\sigma(F)$ and $R_1 = 0.0429$, $wR_2 = 0.0997$, and GOF = 1.082 for all 4382 unique, nonzero reflections and 279 variables. The maximum Δ/σ in the final cycle of least squares was 0.001, and the two most prominent peaks in the final difference Fourier were +0.413 and −0.508 e/Å^3.

Crystals of **4** suitable for X-ray diffraction were crystallized from slow diffusion of a mixture of diethyl ether and cyclohexane into a DMF solution. It was found that the unit cell of **4** contains a molecule of DMF solvent, which refined well, and a second molecule of solvent disordered by the crystallographic center of symmetry, which could not be reliably identified. Three carbon atoms (C21, C22, and C23) were refined isotropically. The weighting scheme used during refinement was $w = 1/[\sigma^2(F_o^2) + 0.0458P^2 + 2.0212P]$ where $P = (F_o^2 + 2F_c^2)/3$. Refinement of **4** converged to $R_1 = 0.0535$ and $R_2 = 0.1139$ for 3268 reflections for which $F > 4\sigma(F)$ and $R_1 = 0.0621$, $wR_2 = 0.1185$, and GOF = 1.146 for all 3682 unique, nonzero reflections and 233 variables. The maximum Δ/σ in the final cycle of least squares was 0.000, and the two most prominent peaks in the final difference Fourier were +0.494 and −0.673 e/Å^3.

Results

Syntheses. $MoOCl_3$(tmazH) (**1**) was prepared following the reported procedure[3] (eq 2). The isolated product **1** reproduced

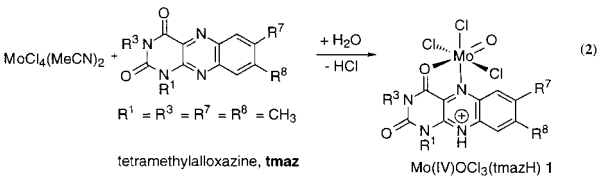

some of the spectral characterizations made in the original report. However, a more extensive investigation of the reactivity of **1** in a variety of solvents shows complicated behavior. $MoOCl_3$(tmazH) (**1**) was structurally characterized by X-ray diffraction and its ORTEP is shown in Figure 1.

Table 1. Electronic and Infrared Spectral Data for **1**, **2**, and **3**

	1	**2**	**3**
	UV/vis, nm (ϵ, mol L^{-1} cm^{-1})		
MeCN	320 (8310)	330 (6400)	314
	388 (7130)	394 (5000)	394
	530 (2740)	564 (4300)	570
acetone	334 (7080)		332
	392 (6770)	398 (4200)	398
	524 (3880)	544 (3700)	570
DMF	318 (8000)	330 (5970)	312
	384 (7100)	406 (2190)	
	626 (1600)	630 (3480)	616
	754 (2200)	768 (sh)	774
DMSO	328	338	*a*
	386	416	*a*
	626	638	*a*
	758	762	
	IR, cm^{-1}		
ν(Mo=O)	982	992	982
ν(CO,CN)	1730	1638	1643
	1609	1609	1599
		1561	1561

[a] Complex **3** rapidly decomposes in DMSO.

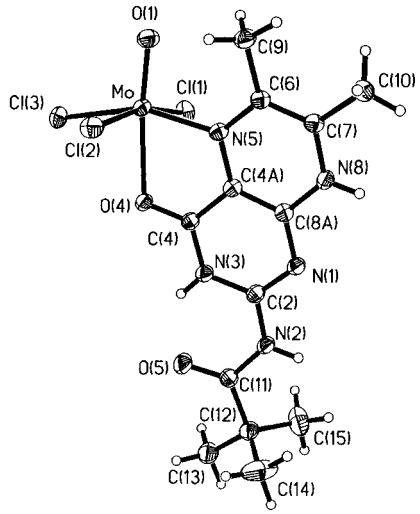

Figure 2. ORTEP diagram of the molecular structure of $MoOCl_3$(piv-dmpH)·EtOEt (**2**) with thermal ellipsoids at 30% probability.

The preparative method for the synthesis of **1** was applied to reactions of $MoCl_4(NCMe)_2$ with other oxidized pterins (piv-dmp and dmp) (eq 3). The Mo−pterin products are spectro-

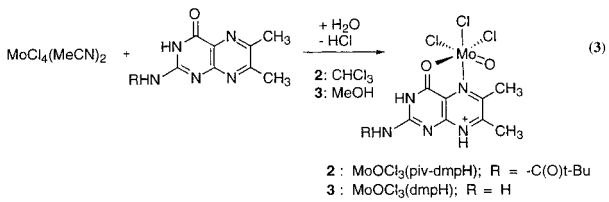

scopically similar to **1** where they exhibit strong MLCT absorptions in the UV/vis spectrum and a familiar pattern of pterin absorptions in the infrared spectrum (Table 1). One of these, $MoOCl_3$(piv-dmpH) (**2**), was also structurally characterized by X-ray diffraction, and its ORTEP is shown in Figure 2.

Complex **3** is especially interesting since it represents the oxidized pterin analogue of the reduced pterin complex $MoOCl_3(H_3dmp)$ (**4**) previously reported.[5b] The X-ray structure of **4** is included here to permit bond distance comparisons between this redox-related pair of molybdenum−pterin complexes **2** and **4**.

Table 2. Crystallographic Data for $MoOCl_3$(HTMAZ) (**1**), $MoOCl_3$(Hpiv-dmp)·EtOEt (**2**), and $MoOCl_3$(H_4dmp)·DMF (**4**)

	1	**2**	**4**
formula	$MoC_{14}H_{15}N_4O_3Cl_3$	$MoC_{17}H_{28}N_5O_4Cl_3$	$MoC_{11}H_{19}N_6O_3Cl_3$
formular weight	489.59	568.73	485.61
space group	$P2_1/n$ (#14)	$P2_1/c$ (#14)	$P\bar{1}$ (#2)
a, Å	8.6460(12)	13.4210(5)	10.0921(4)
b, Å	10.247(2)	16.3960(10)	13.0079(7)
c, Å	21.518(3)	12.4180(4)	8.9545(4)
α, deg			94.312(2)
β, deg	100.880(10)	117.420(3)	104.518(3)
γ, deg			75.261(3)
V, Å^3	1872.1(5)	2425.6(2)	1100.46(9)
Z	4	4	2
ρ(calcd), g cm^{-3}	1.737	1.557	1.466
μ(Mo Kα), cm^{-1}	11.50	9.03	9.79
temp, K	295	233	295
radiation		Mo Kα ($\lambda = 0.71069$ Å)	
$R(F)$, %	8.33	4.29	6.21
$R(wF^2)$, %	18.95	9.97	11.85

In eqs 2 and 3 the incorporation of an oxo group into the coordination sphere of the molybdenum is dependent upon trace water in the solvent. This requirement is supported by the observation that the reaction does not proceed to completion when the solvent is dried with molecular sieves. Purification of **1**, **2**, and **3** can be difficult due to the coprecipitation of unreacted pteridine ligand, and the removal of unreacted pteridine from the product is complicated by hydrogen bonding interactions between the free pteridine and the complex. Use of excess molybdenum reagent in the reaction partially circumvents this problem. Chromatography of impure **3** on silica gel successfully removes unreacted dimethylpterin but unfortunately causes product decomposition.

Spectroscopy and Solution Behavior. Infrared spectroscopy on **1**, **2**, and **3** (Table 1) shows that *ν*(Mo═O) appears between 980 and 990 cm^{-1}, a range commonly observed for oxo-Mo(IV) complexes (980−1000 cm^{-1}). The characteristic absorptions for the pterin and tmaz carbonyl and amide groups shift as a demonstrated in many previous studies.[12]

Compounds **1**, **2**, and **3** in common organic solvents (Table 1) display a range of stabilities that deserve a brief description. Dissolution of **1** and **2** in acetonitrile, acetone, or tetrahydrofuran forms a purple solution accompanied by a broad absorption near 540 nm. **1** and **2** show no decomposition in acetonitrile for at least 10 days whereas they dissociate in acetone up to 25% of the pteridine ligand after 6 days (UV/vis, ^{1}H NMR). **1** and **2** are nonelectrolytes in both acetonitrile and acetone according to conductivity measurements. Complex **3** dissolves in acetonitrile or acetone forming a blue solution and displays stability similar to that observed for **1** and **2** in this solvent**.** All of the complexes **1**, **2**, and **3** are considerably more reactive in DMF solution. For example, **2** produces a blue solution in DMF which changes to green and then bleaches to colorless within an hour. The loss of color suggests dissociation of the pterin, and this speculation is supported by ^{1}H NMR studies. **1** dissolved in DMF immediately yields a green solution where 60% of the flavin has dissociated (^{1}H NMR), and **3** in DMF immediately forms a green solution which fades to colorless within 10 min. All complexes decompose rapidly in DMSO and methanol. In DMSO, the initial green color of complex **3** fades to yellow within seconds whereas **1** and **2** require 1 h to degrade from their purple or blue colors, respectively, to green then yellow. The yellow solution ultimately formed in each case indicates oxidation of the molybdenum to the +6 oxidation state.

The molybdenum complexes of oxidized pterin respond to changes in solution acidity or basicity in a manner similar to their reduced pterin counterparts.[5b] The addition of NEt_3 to purple solutions ($\lambda = 540$ nm) of **1** and **2** in acetonitrile and tetrahydrofuran resulted in a change to green (750 nm) and blue (616 nm) solutions, respectively. Subsequent addition of acid returned the color of the solutions to a purple hue (596 nm), but also caused a decrease in the intensity of the absorbance corresponding to decomposition of the complex. Addition of NEt_3 to an acetone solution of **1** or **2** causes decomposition within seconds.

X-ray Structure Determination of $MoOCl_3$(tmazH) (1), $MoOCl_3$(piv-dmpH)·EtOEt (2), and $MoOCl_3$(H_3dmp)·DMF (4). Crystal structures of $MoOCl_3$(tmazH) (**1**), $MoOCl_3$(piv-dmpH)·EtOEt (**2**), and $MoOCl_3$(H_3dmp)·DMF (**4**) were determined to verify the coordination mode of the alloxazine and oxidized and reduced dimethylpterin ligands, respectively. Crystallographic parameters for **1**, **2**, and **4** are listed in Table 2. Bond distances and angles for the three complexes **1**, **2**, and **4** have been collected together in Tables 3 and 4 to facilitate a detailed comparison of bond distances and angles for a $MoOCl_3$ group coordinated by oxidized pterin and reduced pterin ligands. ORTEP drawings of the molecular unit in the three structures are shown in Figures 1−3 while hydrogen bonding interactions in $MoOCl_3$(H_3dmp)·DMF **(4)** are illustrated in Figure 4. The asymmetric unit in each of the three structures consists of one unique molecule. The asymmetric unit of **2** includes one molecule of diethyl ether, and that for **4** includes one molecule of dimethylformamide.

The alloxazine and both the oxidized and reduced dimethylpterin ligands coordinate to the molybdenum through the N5 and O4 atoms as previously observed in most transition metal complexes of ligands in the pteridine family.[12] The geometry around the molybdenum in all three complexes is distorted octahedral, a result of the small bite angle (ca. 75°) of the alloxazine or pterin ligand. Perhaps the most obvious feature of this distortion from octahedral geometry is the angle between the nominally trans O1 and O4 atoms: O1−Mo−O4 ranges from 166° to 173° where the smallest O1−Mo−O4 angle is observed in **4**. While the Mo−O distances to the oxo ligand O1 are consistent in the three complexes, significant differences in the Mo−N5 bond lengths are observed. The Mo−N5 bond is shorter than expected for a simple dative bond and indicates some double bond character in the three complexes **1**, **2**, and **4**. It is significant that the Mo−N5 bonds in the oxidized pteridine complexes **1** and **2** are longer (2.08 Å) than in the reduced pterin complex **4** (2.01 Å) since this distance reports on the amount of electronic delocalization between the molybdenum and pteridine. The shorter Mo−N5 bond length in **4** correlates to a more extensive delocalization as previously observed for a high

Table 3. Selected Bond Distances (Å) in $MoOCl_3$(HTMAZ) (**1**), $MoOCl_3$(Hpiv-dmp)·EtOEt (**2**), and $MoOCl_3(H_4dmp)$·DMF (**4**)

	1	2	4
Mo−O1	1.658(6)	1.650(2)	1.657(3)
Mo−O4	2.235(5)	2.284(2)	2.238(3)
Mo−N5	2.080(6)	2.082(2)	2.013(4)
Mo−Cl1	2.361(2)	2.4244(8)	2.381(2)
Mo−Cl2	2.362(2)	2.3838(8)	2.3672(14)
Mo−Cl3	2.450(2)	2.3790(8)	2.4434(14)
O2−C2	1.202(10)		
O4−C4	1.250(9)	1.243(3)	1.260(6)
O5−C11		1.222(4)	1.233(7)
N1−C1	1.478(9)		
N1−C2	1.383(11)	1.311(4)	1.330(6)
N1−C8a		1.360(3)	1.346(6)
N1−C10a	1.383(9)		
N2−C2		1.371(4)	1.332(6)
N2−C11		1.393(4)	
N3−C2	1.392(11)	1.364(4)	1.372(6)
N3−C3	1.473(10)		
N3−C4	1.352(10)	1.361(3)	1.353(6)
N5−C4a	1.384(9)	1.382(4)	1.356(6)
N5−C5a	1.401(9)		
N5−C6		1.388(4)	1.499(6)
N8−C7		1.378(4)	1.475(6)
N8−C8a		1.354(4)	1.329(6)
N10−C9a	1.385(9)		
N10−C10a	1.317(9)		
C4−C4a	1.409(11)	1.418(4)	1.401(6)
C4a−C8a		1.380(4)	1.420(7)
C4a−C10a	1.395(10)		
C6−C5a	1.402(10)		
C6−C7	1.376(10)	1.375(4)	1.527(7)
C6−C9		1.497(4)	1.533(8)
C7−C8	1.412(10)		
C7−C10		1.494(4)	1.521(7)
C8−C9	1.381(11)		
C8−C11	1.503(11)		
C9a−C5a	1.397(9)		
C9a−C9	1.391(11)		
Hydrogen Bonding Distances between Pterins in $MoOCl_3(H_4dmp)$ (**4**)			
C1−H8	2.623		
C1−H2b	2.597		
N1−H2A	2.211		
O5−H3	2.693		

Table 4. Selected Bond Angles (deg) in $MoOCl_3$(HTMAZ) (**1**), $MoOCl_3$(Hpiv-dmp)·EtOEt (**2**), and $MoOCl_3(H_4dmp)$·DMF (**4**)

	1	2	4
O1−Mo−N5	97.5(2)	98.17(10)	91.8(2)
O1−Mo−O4	169.2(3)	173.45(9)	166.2(2)
O1−Mo−Cl1	98.6(2)	96.30(8)	97.45(14)
N5−Mo−Cl1	88.0(2)	87.16(7)	89.44(12)
O1−Mo−Cl2	103.9(2)	103.71(8)	107.55(13)
N5−Mo−Cl2	158.5(2)	157.92(7)	160.60(11)
C11−Mo−Cl2	87.43(8)	87.55(3)	86.77(6)
O1−Mo−Cl3	92.1(2)	97.54(8)	94.87(14)
O4−Mo−Cl3	80.2(2)	85.02(6)	82.93(10)
C11−Mo−Cl3	169.13(9)	166.15(3)	167.32(5)
C4a−N5−Mo	115.3(5)	114.7(2)	119.0(3)
C5a−N5−Mo	129.5(5)		
C6−N5−Mo		130.1(2)	126.2(3)
N5−Mo−O4	75.4(2)	75.70(8)	74.76(3)
O4−Mo−Cl1	89.3(2)	81.26(6)	85.81(10)
O4−Mo−Cl2	83.6(2)	82.32(5)	85.98(9)
N5−Mo−Cl3	92.3(2)	91.25(7)	82.93(10)
C12−Mo−Cl3	88.38(7)	88.80(3)	86.65(5)
C4a−N5−C5a	115.1(6)		
C4a−N5−C6		115.2(2)	114.9(4)

oxidation state molybdenum binding a reduced pterin. The oxo group appears to lengthen the trans Mo−O4 bond (2.23−2.28 Å) as is commonly observed in mono-oxo metal complexes. The weaker Mo−O4 interaction is also certainly due to the

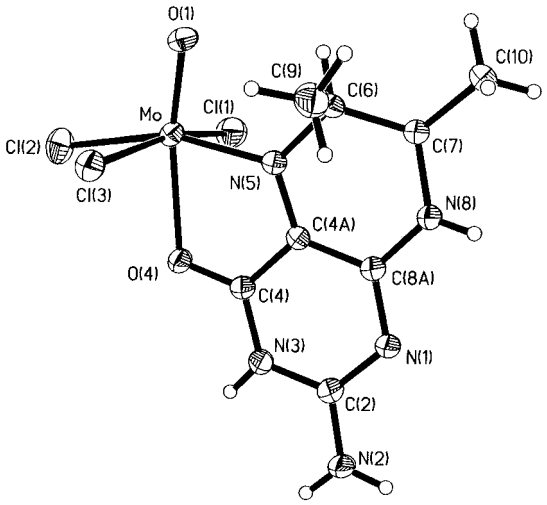

Figure 3. ORTEP diagram of the molecular structure of $MoOCl_3(H_3dmp)$·DMF (**4**) with thermal ellipsoids at 30% probability.

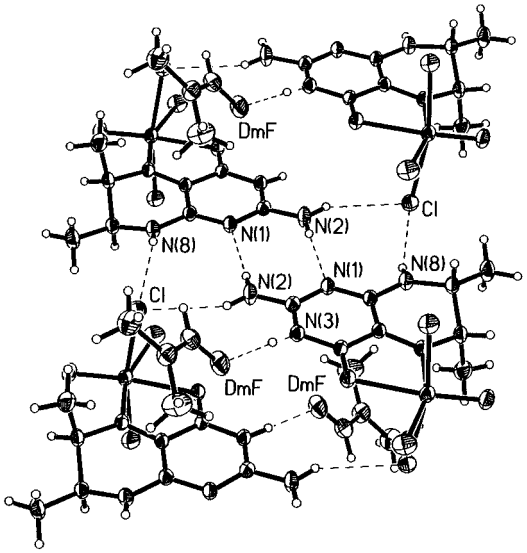

Figure 4. ORTEP diagram illustrating the hydrogen bonding interactions between two molecular units of $MoOCl_3(H_3dmp)$·DMF (**4**).

neutral, as opposed to deprotonated, form of the amide carbonyl C4−O4 (1.2 Å) which limits electron donation. The bond lengths and angles within the pteridine nucleus of the alloxazine in **1** and the pterin in **2** indicate pseudoaromatic delocalization as previously noted in X-ray structures of oxidized pteridines and their metal complexes.[12] All ring atoms of the heterocycle have trigonal planar geometry consistent with an oxidized form of the pteridine. However, in the alloxazine ligand of **1** there is a slight but distinct deviation from ideal planarity. The tmazH ligand is bent approximately 6° along the N5/N10 axis (Figure 5). Dihedral angles between three planes defined by the six atoms in each of the phenyl, pyrazine, and pyrimidine rings are 5.8° between the phenyl and pyrazine rings, 6.2° between the phenyl and pyrimidine rings, and 0.9° between the pyrazine and pyrimidine rings, respectively. The nonplanarity of the tmazH ligand is attributed to its partial reduction. In **2** the carbonyl of the pivaloyl substituent at N2 is oriented forming a third ring held in place by a hydrogen bond between O5 and N3. In contrast to the planar pterin geometry in **2**, the half-chair (or envelope) conformation of the H_3dmp pyrazine ring in **4** is due to the tetrahedral geometry of carbon atoms C6 and C7 and indicates the reduced nature of the H_3dmp ligand. Other indicators of the reduced pterin in **4** are the longer distances

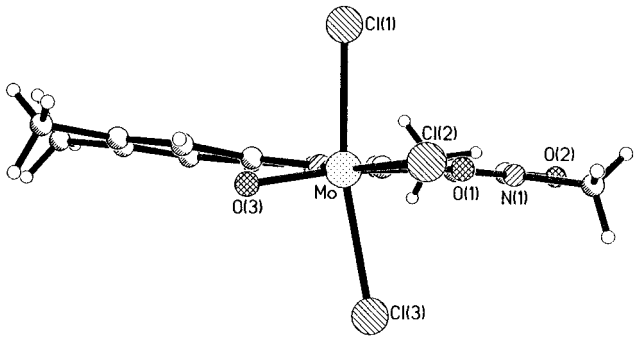

Figure 5. ORTEP diagram illustrating the alloxazine ring bending in $MoOCl_3$(tmazH) (**1**).

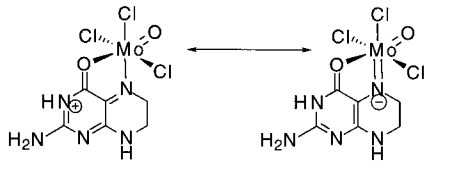

Figure 6. Redox resonance structures illustrating how the formal oxidation state of molybdenum is linked to that of a coordinated, reduced pterin.

N5−C6, C6−C7, and N8−C7 in **4** as compared to **2**. The bond C4a−C8a is considerably lengthened in the reduced pterin in **4** as compared to the oxidized pterin in **2**. This has previously been discussed in the context of partial tetrahydropterin oxidation to quinonoid tautomer of the dihydropterin state.[6b] No hydrogen bonding interactions were observed between molecules in the lattices of **1** and **2**. In complex **4**, however, hydrogen bonding interactions occur between the hydrogens at the N2 and N1 positions on neighboring pterins (Table 2). These interactions are depicted in Figure 4.

Discussion

The most extensive work on metal coordination by flavins was conducted by Hemmerich over 30 years ago.[13] His studies demonstrated that flavin coordination to most divalent metals was not highly favored. This was somewhat surprising considering the structural similarity of flavins and oxine, but Hemmerich attributed the apparent inconsistency to the relatively high pK_a for the amide proton. The claim of flavin coordination to Mo(IV) by Selbin et al. was intriguing in this context.

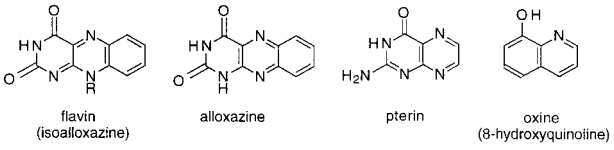

We had a second reason to reinvestigate this Mo−flavin system stemming from our study of redox reactions between molybdenum and pterins. In our previous studies of tetrahydropterin reactions with Mo(VI) complexes, a pair of redox-related resonance structures (Figure 6, structures **A** and **B**) were used to approximate the delocalized nature of the Mo−pterin interaction.[5b] Structure **A** depicts one limiting structure where Mo(IV) coordinates a dihydropterin that is protonated at the amide nitrogen N3. Structure **B** in Figure 6 shows the alternative limiting structure where Mo(VI) coordinates a tetrahydropterin deprotonated at N5. The most accurate view of the molybdenum and pterin oxidation states is a Mo(V)−trihydropterin, an

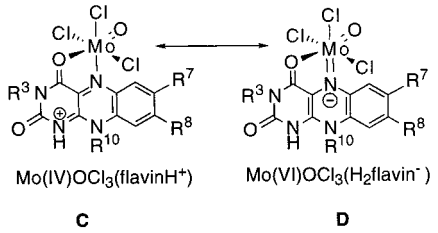

Figure 7. Redox resonance structures for limiting forms of molybdenum coordinated to flavin.

assignment supported by experimental and theoretical data.[5b] Recent XPS results also support this view.[7]

In the structure proposed by Selbin for $MoOCl_3$(flavinH) complexes, the pteridine ligand is specifically protonated at the amide nitrogen N1 (Figure 7, structure **C**). We saw a parallel between the two resonance structures **A** and **B** (Figure 6) and the possibility of a second resonance structure for $MoOCl_3$(flavinH) (Figure 7, structure **D**). Structure **C** represents the oxidized, protonated flavin bound to Mo(IV) as described by Selbin where structure **D** offers the alternative formulation of a deprotonated dihydroflavin chelated to an oxidized Mo(VI) atom. The two-electron redox relationship between the two flavin ligands in **C** and **D** suggested that pterin analogues should be accessible. The analogous pair of species would be Mo(IV) complexed by protonated, oxidized pterin and Mo(VI) coordinated to deprotonated 5,8-dihydropterin. This line of thought initiated our investigations into the reactions of Mo(IV) with the easily synthesized alloxazine tmaz and oxidized pterins dmp and piv-dmp.

An X-ray structure determination of $MoOCl_3$(tmazH) (Figure 1) provides the ultimate proof of its formulation as first described over 20 years ago. Beyond providing confirmation of molybdenum coordination by flavin (and pterin), the X-ray crystal structures of **1** and $MoOCl_3$(piv-dmpH) **2** highlight several key features of transition metals complexed by oxidized pteridine ligands. The first striking feature of these systems is that metal coordination by pteridine is coupled to pteridine protonation. This protonation is additional evidence that electron density has been increased in the pteridine system so that the pteridine is effectively reduced by partial oxidation of the metal. The idea that protonation is coupled to electron delocalization from molybdenum onto the pterin is supported by the solution behavior of the molybdenum−flavin and molybdenum−pterin complexes. While the molybdenum complexes produce relatively stable purple solutions in acetonitrile or acetone, dissolution in a more basic solvent like DMF causes an immediate color change to green followed by rapid bleaching. Similar color changes are observed when triethylamine is added to **1** and **2**. This series of reactions is interpreted as pterin or alloxazine deprotonation at site N8 and N10, respectively, to produce an anionic green species, presumably $[MoOCl_3(\text{pteridine})]^-$, followed by the dissociation of the neutral pteridine, detected by ^{1}H NMR, as signaled by complete bleaching of the solution (eq 4).

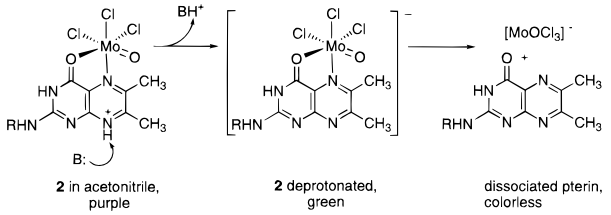

(4)

This hypothesis leads to the prediction that pteridine coordination will be favored under acidic conditions. These observations dovetail nicely with work reported by Clarke et al.[14] where they determined the pK_a's for pterin protons at various positions in several ruthenium−pterin complexes. From these data it was concluded that the site of greatest basicity shifted from N1 to N8 upon coordination of the pterin to the ruthenium. A general conclusion can be made that metal-mediated pterin reduction enables the initial formation of a 5,8-dihydropterin.

The partial pteridine reduction favoring pteridine protonation is further suggested by a structural feature of $MoOCl_3$(tmazH) (**1**). A distinct bending of the flavin along the N5−N10 axis is observed in $MoOCl_3$(tmazH) (Figure 5). Flavin bending was also observed in a ruthenium−flavin complex and used as one of the criteria to support the notion that coordinated flavin was partially reduced and that the ruthenium−flavin complex was best described as a delocalized system of flavinsemiquinone coordinated to ruthenium(III).[15] Applying the same argument to explain the nonplanarity of tmaz in **1** leads to assigned formal oxidation states of Mo(V) and (tmazH$^{\bullet}$) radical. Interestingly, the Mo(V) oxidation state is consistent with XPS data.[7]

The structures of $MoOCl_3$(piv-dmpH) (**2**) and $MoOCl_3$(H_3-dmp) (**4**) offer a unique opportunity to examine the effect of metal coordination on oxidized and reduced tetrahydropterin geometries. The major difference between **2** and **4** is the length of the Mo−N5 bonds. The shorter Mo−N5 bond in **4** corresponds to a greater electron transfer from H_4dmp to Mo(VI) as compared to the electron transfer from Mo(IV) to piv-dmp in **2**. Also significant is the longer C4a−C8a bond in **4**, a result of electron density migrating from the pterin to Mo and the redistribution of π-electron density toward a structure characteristic of the *p*-quinonoid tautomer of dihydropterin.[5a,6b]

The results reported here for molybdenum−pteridine complexes should be put into a larger context. Pteridines join several other redox-active ligands that are well-known for their "noninnocent" behavior in coordination chemistry. All of the ligands exhibit the same preferences with respect to matching ligand and metal oxidation states. In general the reduced and electron-rich form of the ligand (tetrahydropterin,[16] catechol,[17] dithiolene[18]) reacts most readily with metals in a high oxidation state whereas the oxidized and electron-deficient form of the ligand (pterin, quinone, dithione) reacts with lower valent metals. The complexes formed in either of these two extreme cases are characterized by substantial electron delocation over the redox-active ligand/metal framework as they seek to attain electroneutrality. As a result, they present difficulties for chemists attempting to fit the complexes into specific oxidation state assignments. Although these systems seem to defy those attempts by virtue of their highly covalent interactions, application of X-ray photoelectron spectroscopy is a useful tool for estimating the oxidation level the metal, as will be presented in the following article in this issue.

Conclusion

This work demonstrates that oxidized pterin complexes of molybdenum can be successfully synthesized. It further provides examples in support of electronic delocalization between the transition metal and the pteridine ring system. In the case of the oxidized pteridine system the delocalization is from the metal to the pteridine ligand, an electronic flow opposite in direction to that documented for reduced pterins coordinated to highly oxidized molybdenum. The resultant increased electron density in the pteridine ring is balanced by addition of a proton at one nitrogen atom of the pyrazine ring. The net result is a partial reduction of the oxized pteridine to a 5,8-dihydropterin mediated by a transition metal. It is clear that the assignment of formal oxidation states in these systems conveys a restricted notion of the electronic distribution and it is unsuccessful in describing the true nature of the complex.

Supporting Information Available: A complete list of data collection parameters, refinement data and other crystallographic data, final refined atomic coordinates with esd's, calculated hydrogen positions, anisotropic thermal parameters, bond distances and angles, atomic deviations from calculated least squares planes and views of the unit cell for each compound, and an expanded table of electronic spectral data. This material is available free of charge via the Internet at http://pubs.acs.org.

IC9808798

(18) Barnard, K. R.; Wedd, A. G.; Tiekink, E. *Inorg. Chem.* **1990**, *29*, 8.